Journal of the Optical Society of Korea, Vol. 2, No. 2, September 1998, pp. 74-79

Fiber Fabry-Perot type Optical Current Transducer with Frequency Ramped Signal Processing Scheme

Youngil Park

KOREA Telecom, 62-1, Whaam-dong, Yusung-gu, Taejeon, 305-348, KOREA

Wanseok Seo

Electronics and Telecommunication Research Institute, 161 Kajong-Dong, Yusong-Gu, Taejon, 305-350, KOREA

Chung E. Lee

FFPI Industries, 909 Industrial Blvd., Bryan, Texas 77802, U.S.A.

Henry F. Taylor

Department of Electrical Engineering, Texas AM University, College Station, Texas 77843, U.S.A.

(Received January 5, 1998)

The use of a fiber Fabry-Perot interferometer (FFPI) as an optical current transducer is demonstrated. A conventional inductive pickup coil converts the time-varying current $I(t)$ being measured to a voltage waveform $V(t)$ applied across a piezoelectric strip to which the FFPI is bonded. The strip experiences a longitudinal expansion and contraction, resulting in an optical phase shift $\phi(t)$ in the fiber proportional to $V(t)$. This phase shift is measured using a frequency-modulated semiconductor light source, photodiodes to monitor the reflected light from the FFPI and the laser power, and a digital signal processor. Calibration routines compute $V(t)$ and $I(t)$ from the measured phase shift at a 1 KHz rate. Response to 60 Hz ac over the design range 0-1300A rms is characterized. Transient response of the FFPI transducer is also measured.

I. INTRODUCTION

Considerable effort has been devoted to the development of fiber optic current transducers (CTs) in order to realize benefits of lower life-cycle cost, reduced weight, immunity from electrical pickup, and safety. Most of the effort has centered on the use of bulk magnetooptic (Faraday effect) sensing elements, which have been commercialized by several companies for application in both revenue metering and protective relay applications. However, these units are still relatively expensive to purchase and install.

An alternative approach, termed the interferometric optical current transducer (IOCT), uses a conventional inductive pickup coil as a CT to convert the time-varying current $I(t)$ being measured to a voltage waveform $V(t)$ which modulates light in an all-fiber interferometer. A length of fiber in one arm of the interferometer is wrapped around a piezoelectric cylinder with electrodes on inner and outer walls across which $V(t)$ is applied. The cylinder experiences a radial expansion and contraction which causes a proportional phase shift in the fiber and modulation of the transmittance of the interferometer. By monitoring the optical output from the interferometer with a suitable laser input, $V(t)$ can be determined and related to $I(t)$ by a conversion factor. Versions of the IOCT configured as Michelson [1] and Mach-Zehnder [2] interferometers have been reported.

Advantages of these IOCTs over Faraday-effect CTs include simplicity of the optical arrangement, ease of installation with clip-on or clamp-on pickup coils, and the potential to multiplex a number of CTs with a single laser and signal processor. However, for field use stabilization of the fiber interferometer against the effects of vibration and temperature changes becomes a severe problem, because in the Michelson and Mach-Zehnder configurations both the fiber itself and the optical couplers which serve as beam splitters are very sensitive to environmental perturbations.

The fiber Fabry-Perot interferometer (FFPI) [3,4] is another type of interferometer which can serve as the optical sensing element in an IOCT. The FFPI consists of two internal mirrors of reflectance R separated by a length L of single mode optical fiber, as illustrated in Fig. 1. The FFPI is inherently more compact than the Michelson and Mach-Zehnder configurations because the interferometer itself uses no couplers and because the environmentally sensitive region of the optical fiber can be very short ($\approx$ cm for the FFPI, vs. $\approx$ m for the other interferometers). The absence of couplers and reduced fiber length result in greatly improved environmental stability for the FFPI. This paper reports results of the first experiments on an FFPI used as a CT, and describes a novel digital signal processor suitable for multiplexing of a number of sensors with a single light source.

II. DESCRIPTION OF THE SIGNAL PROCESSOR

The function of the signal processor is to determine the round trip optical phase shift ϕ in the interferometer and relate ϕ to the measurand through a calibration procedure. If the mirror reflectance R in an FFPI is $\ll 1$, as in the present case, the reflected optical power P_{ref} is related to ϕ by

$$P_{ref} = 2RP_{in}(1 + \cos\phi), \quad (1)$$

where P_{in} is the input power [5]. Note that P_{ref} varies from a minimum of 0 to a maximum of $4RP_{in}$ as ϕ changes from 0 to 2π. It is convenient to write ϕ as

$$\phi = \phi_m + \phi_s, \quad (2)$$

where ϕ_m is the phase shift in the interferometer due to the measurand of interest and ϕ_s is the phase shift determined by the frequency ν of the light source, given by

$$\phi_s = 2\pi \Delta L n \nu / c \quad (3)$$

with ΔL the round trip optical path length in the interferometer and c the free-space speed of light. In Eq.(2) cross terms between ϕ_m and ϕ_s have been neglected, which is generally valid if $\phi_m \ll \phi_s$. If ν, ΔL, and P_{in} are known, it follows from eqs. (1)-(3) that ϕ_m can be determined from the measured output power using

$$\phi_m = \cos^{-1}[(P_{ref}/2RP_{in}) - 1] - \phi_s \quad (4)$$

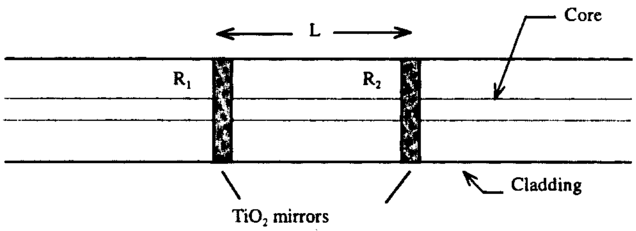

FIG. 1. Fiber Fabry-Perot interferometer (FFPI).

However, in general ϕ_m as described by Eq.(4) is a highly nonlinear function of P_{ref}. When P_{ref} is minimum or maximum, the sensitivity of the interferometer is nullified. Therefore, it is not useful to measure incremental changes of ϕ_m in this case.

Thus, it is generally difficult to measure small phase changes in an interferometer with a high degree of precision using a continuous wave, constant frequency light source. However, with semiconductor lasers which can be tuned by changing the bias current or the heat sink temperature, it is often possible to adjust ϕ_s to a quadrature condition $\phi_s = m\pi \pm \pi/2$, with $m = 0, \pm1, \pm2, \ldots$. At a quadrature point the sensitivity of P_{ref} to changes in ϕ_m is a maximum, and to first order P_{ref} is a linear function of ϕ_m as in Eq.(5).

$$P_{ref} = 2RP_{in}(1 - \phi_m) \quad (5)$$

Operation at quadrature is highly desirable for measurement purposes. However, in cases where optical power for multiple sensors is provided by a single monochromatic laser, simultaneous quadrature operation of all the sensors is not possible. One way to overcome this difficulty is to frequency modulate the laser in periodic fashion with sufficient amplitude that the excursion in ϕ_s is at least π radians. This ensures that the quadrature condition is satisfied for at least one time during each modulation cycle.

A particularly simple digital approach to signal processing is possible if the laser frequency is modulated periodically in sawtooth fashion such that [6]

$$\nu = \nu_0 + \alpha(t - t_n), \quad t_n \le t \le t_{n+1}, \quad n = \text{integer} \quad (6)$$

as illustrated in Fig. 2, where the period of the modulation $T = t_{n+1} - t_n$. The change in ϕ_s during one sawtooth period $\Delta\phi_s$ is determined from Eqs.(3) and (6) to be

$$\Delta\phi_s = 2\pi \Delta L \alpha T / c, \quad (7)$$

and $\Delta\phi_s$ must be at least π radians so that a quadrature point is crossed during each cycle of duration T.

The signal processor determines ϕ_m by measuring the elapsed time from the initiation of the sawtooth

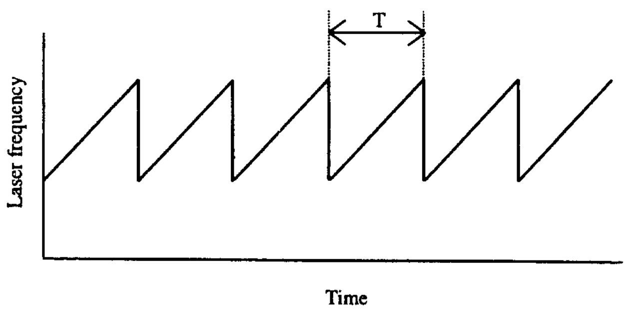

FIG. 2. Ideal linear chirp for laser frequency modulation.

waveform until P_{out} given by Eq.(1) crosses a threshold value P_{th}. In the general case (referring to Eq.(1)) that $P_{in} = P_{in}(t)$, we can choose

$$P_{th}(t) = \beta P_{in}(t) \tag{8}$$

where β is a constant such that $0 < \beta < 2$, and preferably $\beta \approx 1$. Then, from Eqs.(1) and (7), the condition that $P_{out} = P_{th}$ can be written $\phi = \phi_c$, with ϕ_c a constant given by

$$\phi_c = \cos^{-1}(\beta - 1) \tag{9}$$

It then follows from Eqs.(2), (3), and (6) that

$$\phi_m = \phi_c - (2\pi\Delta L/c)[\nu_0 + \alpha(t_{cn} - t_n)], \quad t_n \leq t_{cn} \leq t_{n+} \tag{10}$$

where t_{cn} is the time during the n'th sawtooth ramp that the threshold crossing occurs. The temporal variation of the interferometer output power P_{ref} and the threshold power P_{th} (proportional to the laser power) are illustrated schematically in Fig. 3. Changes in the measurand affect ϕ_m, causing the fringe pattern to shift laterally such that t_{cn} varies linearly with ϕ_m.

To implement the algorithm, a timed counter(clock) is started when the sawtooth is initiated ($t = t_{cn}$) and stopped when a threshold crossing occurs ($t = t_{cn}$). The elapsed time $t_{cn} - t_n$ is then substituted into Eq.(10) to calculate ϕ_m. It is assumed that all of the constants in Eq.(10) have been previously measured or determined by a calibration procedure. Thus, one value for ϕ_m is determined for each modulation cycle of duration T. The measurand of interest is generally proportional to ϕ_m by a calibration constant. The bandwidth of the signal processor is equal to $1/(2T)$.

One of the key aspects in practical implementation of this scheme is in ensuring that the laser frequency change is linear with time as required by Eq.(6) and illustrated in Fig. 2. When a semiconductor laser is current-modulated at frequencies below about 50 MHz, the emission frequency ν is modulated as a result of the temperature change in the active region of the device due to current-induced heating [7,8]. However,

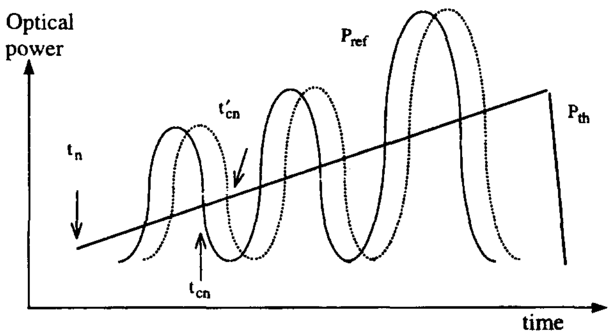

FIG. 3. Principles of the measurement.

the temperature change $\Delta T(t)$ is not a linear function of the modulating current $I(t)$ but depends on the modulation history. In practice $F(\tau)$ is a complicated function and a linear frequency chirp cannot be implemented with a simple step or linear chirp for $I(t)$. In fact, it is clearly not possible to use current modulation of a laser to achieve a linear chirp as described by Eq.(6) for the entire modulation cycle. The greatest nonlinearities tend to occur immediately after the flyback times t_n. The approach taken here is to synthesize a waveform $I(t)$ for which the chirp is linear over most of the period T.

III. SYSTEM IMPLEMENTATION

The FFPI sensing element consists of two internal mirrors separated by a length L of single mode optical fiber, as illustrated in Fig. 1. Any perturbation, which affects the optical path length of the interferometer, causes its reflectance to change. Each mirror is produced by vacuum deposition of a thin film of the dielectric material TiO_2 on the cleaved end of a fused silica (SiO_2) fiber [3,4]. Electric arc fusion splicing is used to integrate the mirrors, each of which has a reflectance R of about 5 %, into a continuous length of the fiber. In the present case, L is 2.0 cm.

The system arrangement is illustrated in Fig. 4. Light from a current-modulated 1.3 μm semiconductor laser diode with a single mode fiber pigtail is coupled through an optical isolator to prevent feedback into the laser. The light then passes through a fiber directional coupler, and a portion of the light is incident on the FFPI, which is bonded to a piezoelectric strip. An inductive pickup coil converts the time-varying cur-

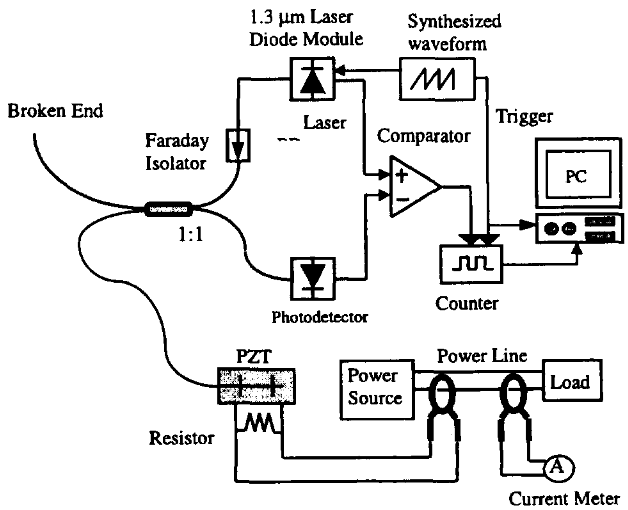

FIG. 4. Experimental arrangement for fiber optic current transducer based upon the fiber Fabry-Perot interferometer

rent $I(t)$ being measured to a voltage waveform $V(t)$ which is applied across the piezoelectric strip, causing the length and hence the reflectance of the FFPI to be modulated. A portion of the reflected light from the FFPI passes through the directional coupler to an InGaAs PIN photodetector in series with a load resistor, which converts the raw optical signal to an electrical signal. A second photodetector converts the optical power from the back facet of the laser to an electrical signal $V_{ref}(t)$. The two voltages $V_{ref}(t)$ and $V_{th}(t)$ serve as inputs to a comparator, which produces a "high" output voltage if $V_{ref} > V_{th}$ and a "low" output otherwise. The signal processor uses a counting procedure to determine the interferometer phase shift, and a personal computer (PC) uses this value to compute $I(t)$.

The laser is modulated repetitively from near its threshold of 30 mA to a maximum current of about 50 mA with a period T of 1 ms, which sets the signal processor bandwidth at 500 Hz. During a cycle the sensor output traverses about 2 1/2 fringes, so $\Delta\phi_s$ in Eq.(7) is $\approx 5\pi$ radians. The round trip optical path length in the interferometer ΔL, equal to twice the interferometer length of 2.0 cm times the fiber refractive index of 1.46, is 5.84 cm. Using these values, it follows from Eq.(7) that the maximum laser frequency change αT is 12.8 GHz. The current waveform for modulating the laser is synthesized by a programmable function generator which consists of a programmable read only memory, a digital to analog converter, and control logic circuits. The current vs. time is calculated from a 7th order polynomial, with coefficients selected to give a nearly linear chirp for the laser output for at least the last 700 μs of the 1 ms period as shown in Fig. 5.

Gains of the two comparator inputs are adjusted so that the two signals $V_{ref}(t)$ and $V_{th}(t)$, which are proportional to $P_{ref}(t)$ and $P_{th}(t)$, cross near the quadrature condition, as in Fig. 3. Each time a crossing occurs, the comparator output changes from "low" to "high" or vice-versa. When each cycle begins (t_n), a trigger pulse is sent by the function generator to initiate the counting routine, which activates an on-chip timer with a 25 MHz clock rate. After a fixed 300 ms dead time to allow the chirp to become linear, the counter interrupt is enabled. Subsequently, the counting is stopped when an appropriate change occurs in the state of the comparator. The accumulated count $t_{cn} - t_n$ is transferred to the PC, where it is multiplied by calibration factors to produce a digital representation of the voltage $V(t)$, which is then integrated to compute $I(t)$. Data from the optical CT are stored in the PC memory along with data from a conventional CT which also monitors $I(t)$.

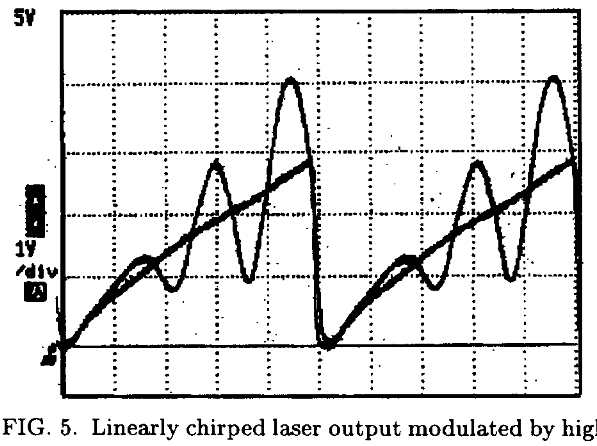

FIG. 5. Linearly chirped laser output modulated by high order polynomial current waveform

IV. EXPERIMENTAL RESULTS

Digital response of the fiber optic CT to 60 Hz ac was characterized using the arrangement of Fig. 4. Output of a conventional current meter was monitored for comparison. Fig. 6 shows the measurement signals when ac current was applied. It is shown that waveforms from the photodetector and the comparator move back and forth. This lateral shift was measured by a counter. With a 75 Ω resistor in parallel with the piezoelectric transducer, the conversion factor from line current I(t) to pickup coil voltage $V(t)$ was found to be 70.0 mV/A. Fig. 7 plots the fiber optic CT output as a function of rms ac current from 0 - 1300 A. Measurements were made for both increasing and decreasing current to check for hysteresis effects, which were found to be small. For currents below 60 A rms the measurement was made directly with the

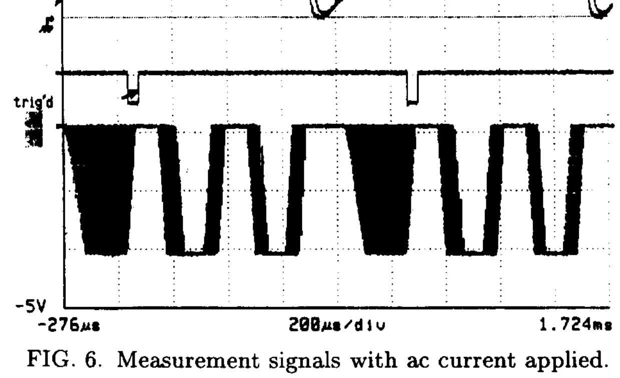

FIG. 6. Measurement signals with ac current applied.

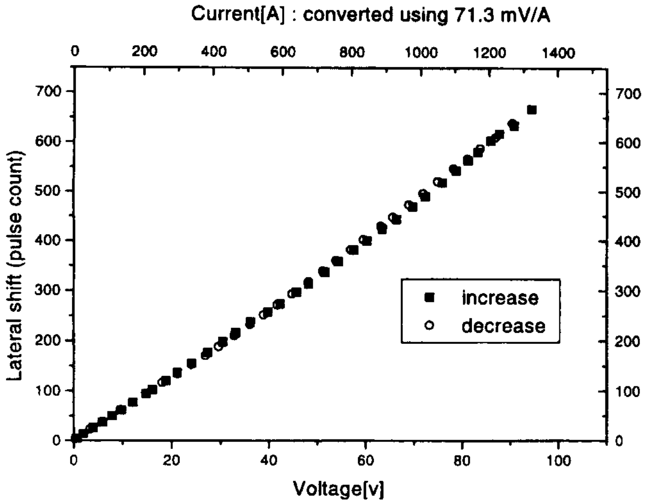

FIG. 7. Digital output of fiber optic CT plotted as a function of ac current amplitude.

arrangement of Fig. 4 ; for higher currents, the pickup coil output was simulated by applying a voltage signal directly to the piezoelectric transducer (PZT). A nonlinearity of about 10 % was observed over the measurement range, which may be attributable to a comparable nonlinearity in the PZT voltage-strain response. This nonlinearity can be compensated using a database or a high order curve equation when the lateral shift is converted to current[Amp] amount.

In the absence of ac ($I = 0$), noise levels of 0.12 % of full scale were observed. These were attributed to mode hopping and partition noise in the multimode laser used in the experiments, and could be reduced through the use of a single mode distributed feedback laser. At current levels above 300 A, the noise was about 0.5 % of current amplitude when averaged over 50 cycles. This noise was attributed to the fact that no effort was made to synchronize the 1 KHz sampling clock with the 60 Hz ac being monitored, so that the sampling points did not exactly coincide with the extrema of the ac waveform. This noise could be greatly reduced by increasing the sampling rate - sampling at 5-10 KHz is readily achievable - or by sampling in phase with the ac waveform. Transient response was studied because several tens of KHz bandwidth is required for protection purposes. Because the pickup coil doesn't require heavy insulation, the frequency response of it can be made high by introducing a small iron core or airgap. The signal processing part can catch up with high frequency by sampling at high rate. Thus, only the transient response of the sensor head was measured since the total system bandwidth is decided by this factor. A piezoelectric strip has its own eigenfrequency which is dependent on the type of the PZT, its physical shape and size. To find this upper frequency limit, a voltage step $V(t)$ was applied to the PZT and the optical response of the FFPI was measured. In that case, the laser frequency was adjusted so that the interferometer operated at a quadrature point. The 10 - 90 % response time was 25 μs, limited by the circuit RC time constant. It satisfies the required specification of a CT to be used for protection. Even faster response can be achieved by a smaller PZT because the resonance frequency of a PZT depends on its dimension.

V. SUMMARY AND CONCLUSIONS

A new optical CT has been implemented using a fiber Fabry-Perot interferometer (FFPI) bonded to a piezoelectric strip as the sensing element. A conventional inductive pickup coil converts the time-varying current $I(t)$ being measured to a voltage waveform $V(t)$ which is applied across a piezoelectric strip to which the FFPI is bonded. The optical phase shift in the FFPI produced by the voltage $V(t)$ is monitored using a frequency modulated laser light source and a novel digital processing scheme. The laser is modulated with a repetitive, nonlinear current waveform to produce a chirped output in which the optical frequency is a nearly linear function of time over most of a modulation cycle. The signal processor determines the interferometer phase shift by a counting procedure which computes the elapsed time from the beginning of a modulation cycle until the optical power from the sensor crosses a threshold value proportional to the laser power. This time of a threshold crossing changes in linear fashion with the interferometer phase shift, which is assumed to be proportional to $V(t)$. The processor multiplies by a calibration factor and integrates to determine $I(t)$. The system has been used to monitor 60 Hz current over the range 0 - 60 A rms, and to simulate currents to 1300 A. Transient response of the FFPI transducer was also measured. Compared to earlier IOCTs, the FFPI is much smaller, less subject to the effects of vibration and temperature changes, and potentially less expensive. The signal processing scheme is designed to accommodate multiplexed operation of a large number of CTs with a single laser and signal processor. Multiplexing should prove cost-effective in measuring current in 3-phase systems and in generation and switching sites where a number of high-voltage lines are present.

REFERENCES

[1] Y. N. Ning, C. B. Chu, and D. A. Jackson, Opt. Lett. **16**, 1448 (1991).

[2] C. M. Davis, EPRI Final Report EL-7421, Research Project 2734-3, Herndon, VA: Optical Technologies, Inc. , (1991).

[3] C. E. Lee and H. F. Taylor, Electron. Lett. **24**, 193 (1988).

[4] R. A. Atkins, J. H. Gardner, W. N. Gibler, C. E. Lee, M. D. Oakland, M. O. Spears, V. P. Swenson, H. F. Taylor, J. J. McCoy, and G. Beshouri, Appl. Opt. **33**, 1315 (1994).

[5] J. J. Alcoz, C. E. Lee, and H. F. Taylor, IEEE Trans. on Ultrasonics, Ferroelectrics, and Freq. Control **37**, 302 (1990).

[6] R. Sadkowski, C. E. Lee, and H. F. Taylor, Appl. Optics **34**, 5861 (1995).

[7] S. Kobayashi, Y. Yamamoto, M. Ito, and T. Kimura, IEEE J. Quantum Electron. **QE-18** 528 (1982).

[8] L. Goldberg, H. F. Taylor, and J. F. Weller, Electron. Lett. **17**, 497 (1981).